The 9th European Congress on Computational Methods in Applied Sciences and Engineering
ECCOMAS Congress 2024
3 – 7 June 2024, Lisboa, Portugal

META-MODEL ASSISTED PATTERN RECOGNITION FOR REAL-TIME IDENTIFICATION OF ROADWAY BRIDGES: A PRELIMINAR STUDY

E. TOMASSINI[*1], E. GARCÍA-MACÍAS[2], I. VENANZI[1] AND F. UBERTINI[1]

[1] Department of Civil and Environmental Engineering
University of Perugia
Via G. Duranti 93, 06125 Perugia, Italy
e-mail: elisa.tomassini@dottorandi.unipg.it

[2] Department of Structural Mechanics and Hydraulic Engineering
University of Granada
Campus de Fuentenueva s/n, 18071 Granada, Spain

Key words: Bridges, Damage identification, Model updating, Operational Modal Analysis, Surrogate models, Structural Health Monitoring.

Summary. In the realm of Structural Health Monitoring (SHM), much research in recent years has been devoted to automated methods that allow real-time, unsupervised monitoring of structures. When damage occurs, extended monitoring of a structure should include detection, localization, quantification, and prognosis of the residual life. While there is broad consensus on the use of control charts for damage detection purposes, various techniques are found in the literature concerning damage identification, encompassing both localization and quantification. When monitoring is conducted through vibration-based techniques, damage identification typically involves the inverse calibration of finite element models through non-linear optimization, presenting computational challenges incompatible with real-time SHM. Therefore, the identification of high-fidelity surrogate models for real-time model updating based on continuous monitoring data is a challenging task in structural system identification. A surrogate model is a mathematical function or algorithm that approximates the behavior of a structure based on collected data from the actual structure (i.e., accelerations, deformations, displacements) in an inexpensive computational manner. Subsequently, surrogate models can be employed to make predictions about the future structural health of the system based on current and past observations. While surrogate models have been often applied to heritage masonry structures, there is no evidence in the literature regarding the application of these powerful techniques to infrastructures like bridges. To address this gap in the literature, the effectiveness of surrogate models is demonstrated in the case study of a real, in-operation, multi-span Italian roadway bridge.

1 INTRODUCTION

Bridges stand as vital lifelines in our infrastructure network, facilitating transportation and commerce while symbolizing engineering prowess and societal progress. However, the

relentless forces of time, environmental stressors, and unforeseen events pose continuous threats to the integrity and safety of these structures. Unlike cultural heritage buildings, bridges endure constant dynamic loading and exposure to environmental factors, rendering them susceptible to progressive deterioration and unforeseen failures. Recent events in the worldwide context [1-3] underscore the urgency of implementing advanced Structural Health Monitoring (SHM) techniques to safeguard these fundamental infrastructures [4]. Therefore, the governments are starting to increase the investments on infrastructures and to enact new regulations in terms of maintenance [5]. In this context, there is a strong call for collaboration between research entities and infrastructure management authorities in order to enforce the technological transfer of SHM techniques and create real-time bridge monitoring networks all over the countries.

In the framework of vibration-based SHM, Operational Modal Analysis (OMA) [6] techniques offer a promising avenue for assessing the health of bridges in real-time. Indeed, by harnessing ambient vibration data collected under operating condition by mean of permanent sensors installed on the bridge, these techniques allow the extraction of its modal parameters, (i.e. resonant frequencies, mode shapes, and damping ratios). The ability to continuously monitor these parameters provides early warning signs of potential damage, enabling timely intervention and targeted maintenance efforts to mitigate risks and prolong the service life of bridges. Among the many OMA algorithms, one of the most used for real-time monitoring is the covariance-driven Stochastic Subspace Identification (cov-SSI) [7] because of its easy automation capability.

One of the key advantages of applying SHM to bridges lies in its potential to perform a comprehensive assessment of the structure. In this frame, it is worth to recall the classification originally performed by Rytter [8] in which SHM systems are hierarchically divided in four levels of complexity depending on the tasks they address: damage *detection*, *localization*, *quantification* and *prediction* of residual operating life. These levels are hierarchically connected, with each one relying on knowledge of the previous level. While the capability of SHM techniques to accomplish real-time damage detection tasks was widely demonstrated, the localization and quantification tasks still need to be formalized to become widely applicable in a large scale. Indeed, real time damage detection can be performed in a fully data-driven approach, by reconducting the presence of a damage in the structure to persistent changes in the statistical distribution of the modal features by mean of continuously updated statistical distance control charts [9-13]. The localization and quantification tasks require a physics-based approach, including Finite Element Models (FEM). The inverse calibration procedure of a FEM of the structure, also called FEM updating, aims to minimize the mismatch between the FEM response and the experimentally identified modal features by the calibration of the model parameters (e.g. material properties, boundary conditions, connections). Therefore, the localization and quantification task may be performed by matching the altered (damaged) experimentally identified modal features and the ones of the FEM, that will thus be able to highlight the damage-induced variations in the mechanical parameters of the structure [14]. Nonetheless, the model updating procedure can be extremely time and computationally demanding, due to the complexity of some bridges (soil-structure interaction, joint connections between consecutive spans, support conditions, large number of elements composing the bridge, periodic variations of the section). In this field, surrogate-based model updating emerges as a particularly promising approach to bridge SHM, offering computational efficiency and

scalability. The construction of surrogate models trained on a detailed FEM simulation permits to bypass the continuous model updating of the structure and streamline the process of damage assessment. The surrogate models consist in high-dimensional representations of the dynmic response of the bridge, able to create a correspence between the the modal features of the structure and corresponding damage sensitive parameters used in the training. Some successful applications of surrogate-based SHM techniques can be found in literature, demonstrating the capability of surrogate models to aid damage localization and quantification in heritage structures [15-17]. Nevertheless, there are no similar experiences in the literature regarding applications to bridge structures.

This paper proposes a preliminary study and discussion on the main steps and issues involved in the construction of surrogate models of a bridge. The steps are reported in detail in Section 2. Then, an application on the case study of the Viaduct over the Corno river (Italy) is proposed in Section 3. The paper concludes with some considerations on the broader implications and future directions of this research endeavor.

2 THEORETHICAL BACKGROUND AND METHODOLOGY

2.1 Surrogate modeling

In essence, the goal of a surrogate model (SM) is to offer a computationally efficient alternative to a high fidelity model in the process of continuous model updating of a structure for damage localization and quantification purposes. Of specific interest to this paper are SMs that can capture the intricate relationship between the variations of the modal features of the structures and specific damage-sensitive parameters. Let us consider a vector $\mathbf{x} = [x_1, \dots, x_m]^{\mathrm{T}}$, where $x_i \in \mathbb{R}$, $i = [1, \dots, m]$ represent the selected damage-sensitive parameters of the structure deployed on the FEM. Denoting with y the response of the FEM (e.g. in terms of natural frequencies, mode shapes and so on), the role of the surrogate model is that of creating a representation of the model's behavior in the form $y(\mathbf{x})$. The creation of the surrogate model includes the following steps:

- *Sampling of the design space:* The first stage is that of generating a dataset comprising N samples of input parameters $\mathbf{x}_j$, $j = [1, \dots, N]$ generated through direct Monte Carlo simulations using the FEM. It is a fundamental requirement to select the boundaries of each design variable to create a subspace $\mathbb{P} = \{\mathbf{x} \in \mathbb{R}^m : a_i \leq x_i \leq b_i\}$ on which to define the sampling population. Therefore, the design matrix is $\mathbf{X} = [\mathbf{x}_1, \dots, \mathbf{x}_N] \in \mathbb{P}^{m \times N}$.
- *Definition of the training population*: The FEM model is run several times to associate its response to each sample previously defined in the design space and so to create the observation vector $\mathbf{Y} = [y_1, \dots, y_N]^T$, where $y_j \in \mathbb{R}$ denotes the FEM's response to the input sample $\mathbf{x}_j$.
- *Construction of the surrogate model*: The previously defined training population is used to train the selected surrogate model. Many different surrogate models can be found in literature, such as response surface method and Kriging model [15]. Let us consider the case in which l mode shapes sampled by n_{dof} degrees of freedom are employed. In that case, a total of $l(1 + n_{dof})$ surrogate models must be developed, encompassing l models for representing the resonant frequencies and $l \cdot n_{dof}$ models for representing the

modal amplitudes.

- *Validation of the surrogate model*: To validate the performance and the accuracy of the comprehensive meta-model, it is worth creating a second design sample defined in the same space $\mathbb{P}$ for comparation purposes between the prediction of the surrogate model and the FEM's results.

Finally, the surrogate model can be used to continuously fit the structural response characteristics (in the present case natural frequencies and mode-shapes) continuously identified on the structure and track the damage-sensitive parameters used in the SM in real-time. It is worth noting that this whole procedure does not take into account some steps that are usually considered in data-driven damage detection, such as the contribution of environmental effects. Therefore, the tracked damage sensitive parameters of the meta-model will be affected by fluctuations due to temperature and humidity.

2.2 Kriging model

The Kriging model originates from Geostatistics applications [18] and consists in a widely adopted interpolation method for spatial data. Here the response function $y(\mathbf{x})$ is defined as:

$$y(\mathbf{x}) = y_r(\mathbf{x}) + F(\mathbf{x}) \tag{1}$$

where $y_r(\mathbf{x})$ is a regression model offering a broad approximation of the design space, while $F(\mathbf{x})$ is a stochastic function *w*ith a zero mean introducing localized fluctuations.

The relation between the interpolated values $\hat{y}(x)$ of the response $y(x)$ at an arbitrary design site x is established by the Kriging predictor:

$$\hat{y}(\mathbf{x}) = \mathbf{f}(\mathbf{x})^{\mathrm{T}}\,\boldsymbol{\beta} + \mathbf{r}(\mathbf{x})^{\mathrm{T}}\,\mathbf{R}^{-1}\,[\mathbf{Y} - \mathbf{f}(\mathbf{x})^{\mathrm{T}}\boldsymbol{\beta}] \tag{2}$$

where: $\boldsymbol{\beta} = [\beta_1, \dots, \beta_p]$, and $\mathbf{f}(x) = [f_1(x), \dots, f_p(x)]^T$, $f_i: \mathbb{R}^m \to \mathbb{R}$ are the regression parameters and functions on which the regression function $y_r(\mathbf{x})$ depends; $\boldsymbol{r}(\mathbf{x})$ represents a vector containing the correlations between the design sites and $\mathbf{x}$, expressed as $\mathbf{r}(\mathbf{x}) = [r(\boldsymbol{\theta}, \mathbf{x}_1, \mathbf{x}), \dots, r(\boldsymbol{\theta}, \mathbf{x}_m, \mathbf{x})]$; $\mathbf{R}$ denotes an $N \times N$ symmetric, positive definite matrix with elements $R_{ij} = \boldsymbol{r}(\boldsymbol{\theta}, \mathbf{x}_i, \mathbf{x}_j)$; $\boldsymbol{\theta}$ represents the vector of correlation parameters.

Consequently, upon determination of the regression model and correlation function, the Kriging interpolator is constructed by selecting appropriate regression parameters β and correlation parameters $\boldsymbol{\theta}$.

3 APPLICATION ON A CASE STUDY AND DISCUSSION

3.1 The bridge

The Viaduct over the Corno river is a three-spans pre-stressed concrete girder bridge located in the center of Italy, in the Umbria region. Each span is 35 m long and is composed by four simply supported I-shaped girders connected by transversal diaphragms on the two heads and in the middle. Overtaking an orographic discontinuity at the base of which the Corno River flows, the two central piers have heights of 16.5 and 19.2 m. The bridge is part of a two-way

road passing through the Italian Appennine mountains, in the area between the rural villages of Norcia and Spoleto. A permanent monitoring system consisting of 21 MEMS accelerometers (±2 g, 24-bit ADC, noise density 22.5 μg/√Hz) strategically placed on the structure is installed on the bridge. Specifically, 6 uniaxial accelerometers were placed on each span in the vertical direction on the inner face of the edge beams at 1/4, 1/2, and 3/4 of the length, respectively. Biaxial accelerometers were also arranged at the head of the two piers in the longitudinal and transverse directions, and a triaxial accelerometer was placed on top of the abutment on the right side of the bridge (Fig. 1). The monitoring system comprises a wired connection to the onboard computer, continuously storing 12 acceleration files per day, 60 minutes long, recorded at a sampling acquisition frequency of 125 Hz.

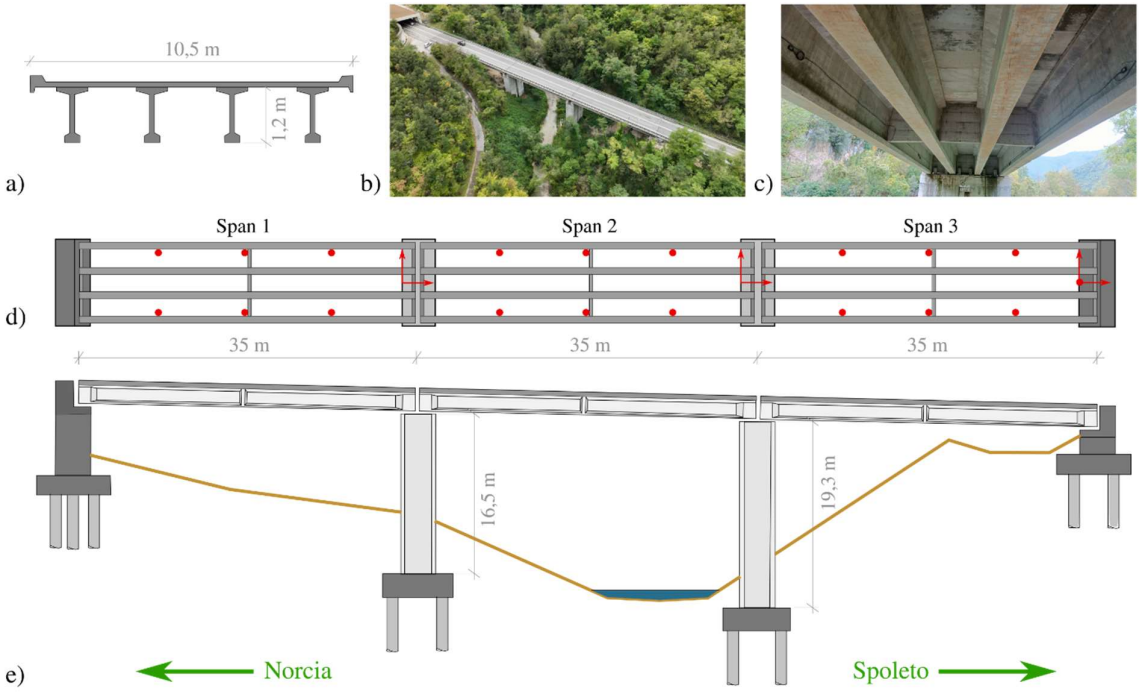

Figure 1: Viaduct over the Corno river. a) Cross-section. b) Picture of the entire bridge. c) Picture of the girders. d) Instrumentation set-up. e) Longitudinal drawing of the bridge.

3.2 Modal identification

To find the resonant frequencies and mode shapes of the bridge, a one-hour acceleration time history recorded on November 9th, 2023, at 10:30 a.m. was analyzed. To automate the modal identification procedure, the covariance-driven Stochastic Subspace Identification [11] was used. Specifically, main parameters considered in the algorithm included a time-lag of 3.2 seconds and the stabilization diagram was determined considering model orders ranging from 40 to 200. Some soft criteria for spurious modes removal were applied between each pair of poles i and j identified at model orders m and $m-1$, including $(f_i^m - f_j^{m-1})/\max(f_i^m, f_j^{m-1}) \leq 1\%$,

$MAC(\phi_i^m, \phi_j^{m-1}) \leq 0.98$, and $(\xi_i^m - \xi_j^{m-1})/\max(\xi_i^m, \xi_j^{m-1}) \leq 5\%$. Additionally, modes with damping $\xi_i \geq 10\%$ and those with Modal Phase Collinearity $MPC \leq 60\%$ and Mean Phase Deviation $MPD \geq 50\%$ were excluded. After stable poles selection, a Hierarchical clustering algorithm was used to finally identify the physical mode shapes of the structure. The first 4 resonant mode shapes (that will be used in Section 3.3 to calibrate the FEM) are reported in Fig. 2 and the corresponding frequencies are reported in the second column of Table 2. The identified mode shapes, showing the 1st order bending and torsional modes of the deck, highlight a strong coupling between the 2nd and 3rd spans, while the 1st one presents a more independent behavior. *Mode 1* and *Mode 2* are the 1st order bending modes of spans 2 and 3. *Mode 3* represents the 1st order torsional mode of spans 2 and 3, with some bending modal contribution of the 1st span. Finally, *Mode 4* is the 1st order bending mode of Span 1.

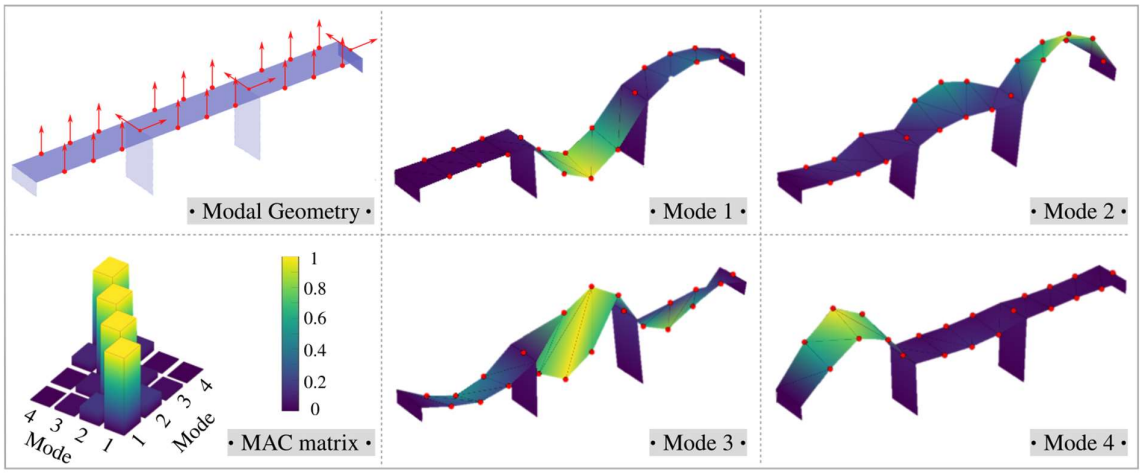

Figure 2: Experimentally identified mode shapes of the Viaduct over the Corno river.

3.3 FEM calibration

A FEM model was built using SAP2000® software. The goal of the FEM was not to achieve a high fidelity digital twin of the real structure but to replicate the structure's behaviour as accurately as possible while maintaining high computational efficiency. Therefore, both the piers and beams were modelled using beam elements, while the concrete slab was modelled using shell elements. To maintain a constat curvature on the section of the deck, each node on the slab was linked to the beam with infinitely rigid perpendicular link elements. To introduce a partial coupling between spans, four rotational springs were used to connect the beams of contiguous spans in correspondence to the joints. Indeed, despite the visible joints in the slab and the girders being simply supported on the piers, the experimental modal shapes show clear coupling not solely due to the piers' oscillation.

The girders of each span are bounded by fixed supports on one side and movable supports in the longitudinal direction on the opposite side. Specifically, the fixed supports of Spans 1, 2

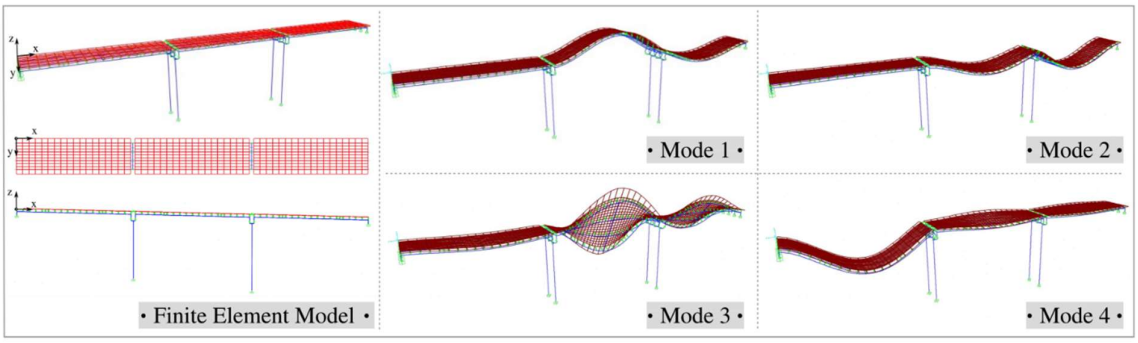

Figure 3: Calibrated Finite Element Model of the Viaduct over the Corno river.

and 3 were deployed on the first abutment, second pier and second abutment, respectively. After some manual tuning, all the supports were fixed in transversal direction while their rotational stiffnesses were included in the calibration. The soil-structure interaction was not considered in the modelling phase, so fixed constraints were assigned at the base of each pier. While this choice is not optimal from the physical point of view, it is capable to optimizing the computational burden of the analysis bypassing the uncertainties of soil-pile modelling. Finally, the following 29 model parameters were calibrated:

- The stiffnesses and masses per unit volume of the girders (E_{G1}, E_{G2}, E_{G3}, ρ_{G1}, ρ_{G2}, ρ_{G3}), slabs (E_{S1}, E_{S1}, E_{S1}, ρ_{S1}, ρ_{S1}, ρ_{S1}) and transversal diaphragms (E_{T1}, E_{T1}, E_{T1}, ρ_{T1}, ρ_{T1}, ρ_{T1}) of the three spans;
- The rotational stiffnesses of the springs at the joints between Spans 1 and 2 ($r_{J,12}$), and between Spans 2 and 3 ($r_{J,23}$);
- The rotational stiffnesses of the fixed supports of the three spans ($r_{F,1}, r_{F,2}, r_{F,3}$);
- The longitudinal ($k_{M1}, k_{M,2}, k_{M,3}$) and rotational ($r_{M,1}, r_{M,2}, r_{M,3}$) stiffnesses of the movable supports of the three spans.

The FEM calibration was carried out in several steps, each time considering different model parameters to limit the problem's indeterminacy due to the high number of calibration parame-

Table 1: Calibrated model parameters.

E_{S1}	38356 N/mm^2	E_{G1}	37757 N/mm^2	E_{T1}	37761 N/mm^2
E_{S2}	34438 N/mm^2	E_{G2}	34809 N/mm^2	E_{T2}	38650 N/mm^2
E_{S3}	38285 N/mm^2	E_{G3}	33894 N/mm^2	E_{T3}	31325 N/mm^2
ρ_{S1}	2.47E-09 N/mm^3	ρ_{G1}	2.32E-09 N/mm^3	ρ_{T1}	2.74E-09 N/mm^3
ρ_{S2}	2.81E-09 N/mm^3	ρ_{G2}	2.67E-09 N/mm^3	ρ_{T2}	2.67E-09
ρ_{S3}	2.57E-09 N/mm^3	ρ_{G3}	2.73E-09 N/mm^3	ρ_{T3}	2.62E-09 N/mm^3
k_{M1}	3859 N/mm	$k_{M,2}$	3994 N/mm	$k_{M,3}$	5064 N/mm
r_{M1}	2.5E+10 N/rad	r_{M2}	2.41E+11 N/rad	r_{M3}	4.36E+11 N/rad
$r_{F,1}$	2.78E+13 N/rad	$r_{F,2}$	7.10E+13 N/rad	$r_{F,3}$	4.44E+13 N/rad
$r_{j,12}$	1.42E+12 N/rad	$r_{j,12}$	2.79E+11 N/rad		

Table 2: Model updating results.

MODEL UPDATING RESULTS				
Mode #	$\boldsymbol{f_{Exp}}$ [Hz]	$\boldsymbol{f_{FEM}}$ [Hz]	$\boldsymbol{\Delta f/f_{Exp}}$ [%]	**MAC** [-]
1	4.432	4.325	**-2.406**	**0.890**
2	4.482	4.605	**2.757**	**0.858**
3	5.102	5.112	**0.195**	**0.851**
4	5.341	5.160	**3.391**	**0.947**

ters with respect to available experimental modes. A genetic optimization algorithm was adopted to minimize the following cost function *J*:

$$J\left(\boldsymbol{f_{exp}}, \boldsymbol{f_{FEM}}, \boldsymbol{MAC}\left(\boldsymbol{\Phi_{exp}}, \boldsymbol{\Phi_{FEM}}\right)\right) = \alpha \sum_{i=1}^{4} \frac{f_{\exp}^{i} - f_{FEM}^{i}}{f_{exp}^{i}} + \beta \sum_{i=1}^{4} MAC(\phi_{\exp}^{i}, \phi_{FEM}^{i}) \quad (3)$$

where: $\boldsymbol{f_{exp}}$, $\boldsymbol{f_{FEM}}$ and $\boldsymbol{MAC}\left(\boldsymbol{\Phi_{exp}}, \boldsymbol{\Phi_{FEM}}\right)$ contain the experimentally identified frequencies, the resonant frequencies iteratively derived from the FEM and the MAC value between the experimentally identified mode shapes and the ones iteratively derived from the FEM, respectively; α and β are weight coefficients equal to 0.2 and 0.5, respectively. The final calibrated model parameters are collected in Table 1. The calibration results are shown in Table 2, and the calibrated modes in Figure 3. In Table 1, it is useful to note how the construction of a FEM model with a low computational burden (5 seconds) can lead to disequilibria regarding the optimal parameters and thus to very different values for similar elements. Indeed, given the simplicity of the model, it may happen that the optimal values of these parameters are not able to be completely consistent with each other, as would be the case with a solid model.

3.4 Surrogate model

Starting from the model calibrated in the previous step, a surrogate model was constructed for damage localization and quantification purposes. The main issue here is the large number of damage-sensitive parameters required for the accurate localization, as this would result in excessive indeterminacy of the problem, leading to aliasing, loosing of univocity of the predictions and misclassifications. Therefore, the model was constructed with the simplest possible parameterization to assess whether, even with few parameters, it could be sensitive to different damage scenarios than the parameterization itself. The surrogate model thus includes only three sensitive parameters: the flexural stiffnesses of the girders in the three spans (E_{G1}, E_{G2}, E_{G3}).

To facilitate model interpretation, the three damage parameters were not directly varied but rather through multiplicative coefficients of the calibrated values. Specifically, two three-dimensional sample spaces were generated where the multiplicative coefficients vary between 0.9 and 1.05. The training design space contained 2^{10} samples, and the validation design space contained 2^{8} samples, generated by mean of a Latin hypercube algorithm. The calibrated FEM was then used to produce the training population of the surrogate model. Finally, the Kriging

interpolator was used to construct the 3D surfaces of the meta-model. For this study, Gaussian correlation functions and zeroth-order regression functions have been chosen.
Figure 3 shows a comparison between the predictions of the surrogate model and the FEM model response on the validation design space. It is noteworthy that the surrogate model perfectly matches all four calibrated frequencies, consistently showing an R^2 value of 0.99. Regarding the mode shapes, there is an optimal correspondence in the case of Mode 1 and Mode 2, while larger inaccuracies (probably due to some mode shifting, given the closely spaced frequencies) appear for Modes 3 and 4.

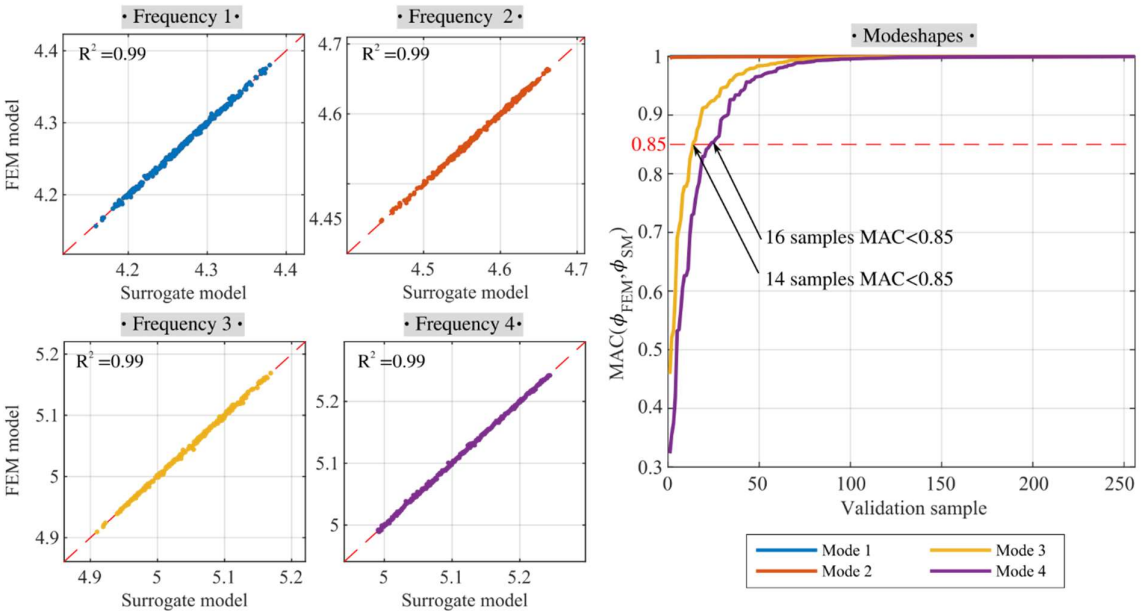

Figure 4: Comparison between the predictions of the surrogate model and results of the FEM on the validation design space.

4 CONCLUSIONS

This work aims to present the various steps involved in constructing a surrogate model to locate and quantify damage in the specific case of multi-span girder bridges and to identify its critical aspects. After an overview of the theoretical background underlying surrogate-based model updating, a Kriging surrogate model based on the calibrated FEM of the Viaduct over the Corno river was generated. This work highlights some difficulties that may arise during the construction of a surrogate model, summarized as follows:

- Calibrating an efficient FEM is not straightforward because the small number of degrees of freedom may not allow the FEM model to easily reproduce experimental frequencies and mode shapes. Therefore, it may be necessary to use markedly different physical

parameters even for similar elements to match the modes extracted from the model with those identified experimentally.

- When the modal frequencies used in the calibration phase are very closely spaced, the variation of the input parameters in the design space can lead to overlapping and mode shifting, resulting in problems with the accuracy of the surrogate model. Thus, it is necessary to use mode matching tools that can recognize the mode shapes and associate them with the corresponding frequency.

- The choice of parameters to be used as damage-sensitive features in the surrogate model is critically important because the model's ability to correctly localize and quantify damage depends on it. Therefore, it is necessary to reduce the level of indeterminacy of the problem as much as possible, considering the limited number of output parameters derived from the frequencies and mode shapes used in the calibration.

- Once the training of the surrogate model is performed, damage assessment can be done quickly and with an extremely low computational burden compared to that generated by continuous model updating.

ACKNOWLEDGEMENTS

The authors acknowledge funding by the Italian Ministry of University and Research (MUR) through the project of national interest "TIMING – Time evolution laws for IMproving the structural reliability evaluation of existING post-tensioned concrete deck bridges" (Protocol No. P20223Y947) and by FABRE – "Research consortium for the evaluation and monitoring of bridges, viaducts and other structures" (www.consorziofabre.it/en) within the activities of the FABRE-ANAS 2021-2024 research program. Any opinion expressed in the paper does not necessarily reflect the view of the funders.

REFERENCES

[1] Calvi, G. M., M. Moratti, G. J. O'Reilly, N. Scattarreggia, R. Monteiro, D. Malomo, P. M. Calvi, and R. Pinho. 2019. "Once upon a time in Italy: The tale of the Morandi bridge." *Structural Engineering International* 29 (2): 198–217.

[2] Zhang, G., Y. Liu, J. Liu, S. Lan, and J. Yang. 2022. "Causes and statistical characteristics of bridge failures: A review." *Journal of Traffic and Transportation Engineering* 9 (3): 388–406.

[3] Apportionment of Highway Infrastructure Program Funds Pursuant to the Department of Transportation Appropriations Act (May 5, 2022). Federal Highway Administration (FHWA) of U.S. Department of Transportation.

[4] An, Y., E. Chatzi, S.-H. Sim, S. Laflamme, B. Blachowski, and J. Ou. 2019. "Recent progress and future trends on damage identification methods for bridge structures." *Structural Control and Health Monitoring* 26: e2416.

[5] Guidelines on Risk Classification and Management, Safety Assessment and Monitoring of Existing Bridges (July 1, 2022). Italian Ministry of Infrastructure and Transport.

[6] Magalhães, F., and Á. Cunha. 2011. "Explaining operational modal analysis with data from an arch bridge." *Mechanical Systems and Signal Processing* 25 (5): 1431–1450.

[7] Reynders, E., J. Houbrechts, and G. De Roeck. 2012. "Fully automated (operational) modal analysis." *Mechanical Systems and Signal Processing* 29: 228-250.

[8] Rytter, A. 1993. *Vibration based inspections of civil engineering structures*. PhD Thesis, Department of Building Technology and Structural Engineering, University of Aalborg, Denmark.

[9] Peeters, B., and G. De Roeck. 2001. "One-year monitoring of the Z24-Bridge: environmental effects versus damage events." *Earthquake Engineering and Structural Dynamics* 30: 149–171.

[10] Yan, A. M., G. Kerschen, P. De Boe, and J. C. Golinval. 2005. "Structural damage diagnosis under varying environmental conditions – part II: local PCA for non-linear cases." *Mechanical Systems and Signal Processing* 19: 865–880.

[11] Magalhães, F., A. Cunha, and E. Caetano. 2012. "Vibration based structural health monitoring of an arch bridge: from automated OMA to damage detection." *Mechanical Systems and Signal Processing* 28: 212–228.

[12] García-Macías, E., and F. Ubertini. 2020. "MOVA/MOSS: Two integrated software solutions for comprehensive Structural Health Monitoring of structures." *Mechanical Systems and Signal Processing* 143: 106830.

[13] Kullaa, J. 2003. "Damage detection of the Z24 bridge using control charts." *Mechanical Systems and Signal Processing* 17: 163–170.

[14] Schommer, S., V. H. Nguyen, S. Maas, and A. Zürbes. 2017. "Model updating for structural health monitoring using static and dynamic measurements." *Procedia Engineering* 199: 2146-2153.

[15] García-Macías, E., I. A. Hernández-González, E. Puertas, R. Gallego, R. Castro-Triguero, and F. Ubertini. 2022. "Meta-Model Assisted Continuous Vibration-Based Damage Identification of a Historical Rammed Earth Tower in the Alhambra Complex." *International Journal of Architectural Heritage* 18 (3): 427–453.

[16] García-Macías, E., I. Venanzi, and F. Ubertini. 2020. “Metamodel-based pattern recognition approach for real-time identification of earthquake-induced damage in historic masonry structures.” *Automation in Construction* 120: 103389.

[17] Cabboi, A., C. Gentile, and A. Saisi. 2017. “From continuous vibration monitoring to FEM-based damage assessment: Application on a stone-masonry tower.” *Construction and Building Materials* 156: 252-265.

[18] Matheron, G. 1963. “Principles of geostatistics.” *Economic Geology* 58: 1246–66.